

Oxygen Fluorescence Quenching Studies with Single Tryptophan-Containing Proteins

Maurice R. Eftink^{1,3} and Camillo A. Ghiron^{2,4}

Received July 12, 1993; revised February 11, 1994; accepted February 15, 1994

The work of Lakowicz and Weber [*Biochemistry* 12, 4161 (1973)] demonstrated that molecular oxygen is a powerful quencher of tryptophan fluorescence in proteins. Here we report studies of the oxygen quenching of several proteins that have a single, internal tryptophan residue. Among these are apoazurin (*Pseudomonas aeruginosa*), asparaginase (*Escherichia coli*), ribonuclease T₁ (*Aspergillus oryzae*), and cod parvalbumin. Both fluorescence intensity and phase lifetime quenching data are reported. By comparison of these data we find that there is a significant degree of apparent static quenching in these proteins. The dynamic quenching rate constants, k_q , that we find are low compared to those for tryptophan residues in other proteins. For example, for apoazurin we find an apparent k_q of $0.59 \times 10^9 M^{-1} s^{-1}$ at 25°C. This value is the lowest that has been reported for the oxygen quenching of tryptophan fluorescence.

KEY WORDS: Oxygen fluorescence quenching; tryptophan fluorescence in proteins; Smoluchowski equation.

INTRODUCTION

It was shown by Lakowicz and Weber [1] that molecular oxygen is able to quench the fluorescence of internal tryptophan (trp) residues in globular proteins, with apparent bimolecular rate constants in the range of $2\text{--}7 \times 10^9 M^{-1} s^{-1}$. This result demonstrates that O₂ can diffuse through the matrix of proteins with a diffusion coefficient that is 20–50% as large as that for diffusion of O₂ through water. It has been argued by Lakowicz and Weber and others [2–4] that this facile diffusion of O₂ must be facilitated by fluctuations in the conformation of the protein on the nanosecond time scale.

Here we have reinvestigated the O₂ quenching of

selected proteins.^{5,6} The reasons for our studies are threefold. First, the pioneering work by Lakowicz and Weber included only one protein that contains a single trp residue. While their conclusion is not doubted, the case would certainly be stronger if O₂ quenching data for a number of single trp-containing proteins were available, for it would then dismiss any alternate explanations of the quenching data (i.e., it would dismiss the possibility that only the surface trp residues are fluorescent in the original study). The O₂ quenching of ribonuclease T₁ and cod parvalbumin, a couple of proteins having single, internal trp residues, has been reported [5–7]. In this article we report O₂ quenching data for other proteins with single trp residues, some of which are internal and some of which are on the surface.

¹ Department of Chemistry, University of Mississippi, University, Mississippi 38677.

² Department of Biochemistry, University of Missouri, Columbia, Missouri 65201.

³ To whom correspondence should be addressed.

⁴ Current address, 2130 North Lincoln Park West, Chicago, Illinois 60614-4639.

⁵ Abbreviations used: D , diffusion coefficient of quencher + fluorophore; F , fluorescence intensity; k_q , quenching rate constant, with O₂ as quencher; λ_{\max} , emission maximum; R_0 , critical interaction radius for quenching reaction; τ , fluorescence decay time.

⁶ A preliminary report of a portion of this work (the data in Fig. 1) appeared in Ref. 7.

Second, the O₂ quenching experiments are lengthy due to the slow equilibration of the gas with an aqueous solution. Previously we reported an improved experimental procedure, which greatly reduces the time needed for the experiments [8]. With the increased speed and with the excellent stability of present fluorescence lifetime equipment, we can now obtain intensity and lifetime quenching data for an aqueous sample in 1–2 h.

Third, the existence of apparent static quenching by O₂ in protein systems needs to be investigated further. (By apparent static quenching we mean the observation that an intensity Stern–Volmer plot has a larger slope than a lifetime Stern–Volmer plot, and/or the intensity plot is upward curving.) Previous studies have indicated that static O₂ quenching of internal trp residues does occur [1,6]. Lakowicz *et al.* [9] have presented data that indicate that the transient term of the Smoluchowski equation (or the radiation boundary model) can be used to describe the kinetics of the quenching of iodide and acrylamide of indoles in aqueous solution. Also, Lakowicz *et al.* [10] have presented data that indicate that the transient term is also important in fitting acrylamide and oxygen quenching of trp fluorescence in proteins, where time-resolved fluorescence intensity data are considered. Simulations show that such a transient Smoluchowski term will result in an upward curving steady-state intensity Stern–Volmer plot and that a plot of F_0/F (fluorescence intensity in the absence and presence of quencher) versus [quencher] will have a larger slope than a plot of τ_0/τ (where τ is a phase lifetime at a single modulation frequency) [11]. In other words, a transient Smoluchowski term will result in an apparent static quenching process. In this article we introduce a procedure for simultaneously fitting a transient model to both steady-state intensity and phase lifetime quenching data.

MATERIALS AND METHODS

Materials. Ribonuclease T₁ from *Aspergillus oryzae* was generously provided by Dr. Frederick Walz, Kent State University. Azurin from *Pseudomonas aeruginosa* was generously provided by Dr. David Jameson, University of Hawaii, and the Cu²⁺ was removed according to the procedure of Blaszkak *et al.* [12]. Nuclease A from *Staphylococcal aureus* was provided by Dr. R. O. Fox, Yale University. Parvalbumin was purified from codfish, as described previously [6]. Monellin (*Dioscoreophyllum cumminsii*) and asparaginase (*Escherichia coli*) were obtained from Sigma Chemical Co. fd phage

was generously provided by Dr. R. Webster, Duke University. *N*-Acetyl-L-tryptophanamide (NATA) was obtained from Sigma Chemical Co. All buffers were prepared with distilled, deionized water. The buffers for each protein are given in Table I.

Fluorescence lifetime and intensity measurements were made with a SLM 4800 phase/modulation fluorometer, which has been modified to operate at multiple frequencies with an ISS, Inc., package including a Pockels cell modulator, 250-MHz synthesizers, and a 300-W xenon lamp. A modulation frequency of 50 MHz was used for most lifetime measurements. Excitation was at 290 nm (selected via a 10-nm interference filter); emission was collected through bandpass filters. *p*-Terphenyl was used as a reference compound ($\tau = 1.0$ ns).

A high-pressure cell, following the design of Lakowicz and Weber [13], was kindly loaned to us by Dr. David Jameson, University of Hawaii. The cell holder was temperature regulated via an external, circulating water bath. Measurements were made at 20°C, unless indicated otherwise.

Table I. Diffusion Coefficients for Oxygen Fluorescence Quenching Reactions^a

	τ_0 (ns)	$D \times 10^5$ (cm ² /s)
Apoazurin	3.59 ± 0.04	0.14 ± 0.02
Asparaginase	2.18 ± 0.01	0.161 ± 0.005
Ribonuclease T ₁	2.90 ± 0.02	0.344 ± 0.008
Parvalbumin	3.49 ± 0.07	0.39 ± 0.02
Nuclease A	4.55 ± 0.26	0.45 ± 0.07
fd phage	3.29 ± 0.03	0.49 ± 0.02
Monellin	3.00 ± 0.03	1.03 ± 0.03
Adrenocorticotropin	2.24 ± 0.04	1.75 ± 0.06
NATA		
15°C, 45% glycerol	3.74 ± 0.04	0.51 ± 0.02
15°C	3.22 ± 0.07	1.85 ± 0.05
25°C	2.75 ± 0.04	2.03 ± 0.05 (2.0) ^b

^aFitting parameters obtained from analysis of intensity and raw phase lifetime (50-MHz) data via Eqs. (2)–(6), the Smoluchowski model. The value of R_0 was fixed at 5.5 Å and the decay time was assumed to be a monoexponential, described by decay time τ_0 in the absence of quencher. The buffer used was 0.03 M sodium phosphate at pH 7.2 for all proteins, except parvalbumin, where the buffer was 0.1 M Tris–HCl, pH 8.0. The temperature was 20°C, unless indicated.

^bValue determined by analysis of multifrequency phase/modulation data in the presence of O₂ in terms of the Smoluchowski model [Eq. (1)] [10]. Lakowicz *et al.* have also fitted the O₂ quenching of NATA in terms of the radiation boundary condition model (RBC) and have obtained a value of $D = 6.2 \times 10^{-5}$ cm²/s and $\kappa = 505$ cm/s, where κ is the rate constant for the quenching reaction when the quencher is at distance R_0 from the excited fluorophore.

The time it takes to equilibrate a solution with an O₂ pressure is usually quite long (~1 h), even with stirring of the solution. Due to this long equilibration time, a large sample cell (2.5 × 2.5 cm) and a large aqueous volume (~20 ml) is usually used to increase the gas–aqueous surface contact area. The use of a large volume is sometimes a problem when samples are precious and the long equilibration time leads to problems in the long-term stability of the fluorescence measurements. To lessen these problems we have modified the O₂ pressure cell to enable the gas to be bubbled directly through the aqueous sample when O₂ pressure is increased. This procedure is described elsewhere [8]. We use a standard 1 × 1-cm quartz cuvette, to reduce the volume of the sample to about 3 ml. Oxygen concentrations were determined from Henry's law and the following solubilities at 1 atm: 0.001275 M in water at 25°C, 0.00154 M in water at 15°C, and 0.000786 M in 45% glycerol–water (w/w) at 15°C [19].

The simultaneous fitting of steady-state intensity and lifetime data was by a numerical integration procedure as described below. For a quenching process, we assume that the collisional quenching rate constant is given by the Smoluchowski equation

$$k_q(t) = 4\pi R_o D N' (1 + R_o \sqrt{\pi D t}) \quad (1)$$

where R_o is the interaction radius for the quenching reaction, D is the sum of the diffusion coefficients of the fluorophore and quencher, and N' is Avogadro's number per millimole. The time-dependent fluorescence signal, $F(t)$, in the presence of quencher, Q , will then be

$$F(t) = F_o \exp(-t/\tau_o - 4\pi R_o D N' [Q] t (1 + 2R_o \sqrt{\pi D t})) \quad (2)$$

where F_o is the intensity at time t , equal to zero, and τ_o is the fluorescence decay time in the absence of quencher. Thus, in the presence of quencher the fluorescence decay is expected to be nonexponential due to the \sqrt{t} term. Integration of the above impulse-response function gives the steady-state fluorescence intensity, $F_{ss} = \int F(t) dt$. The above equation is related to frequency-domain fluorescence lifetime data in the following way. The phase angle, Θ_ω , and relative modulation, M_ω , measured at modulation frequency ω are given by

$$\theta_\omega = \arctan(N_\omega/D_\omega) \quad (3a)$$

$$M_\omega = (N_\omega^2 + D_\omega^2)^{1/2} \quad (3b)$$

where N_ω and D_ω are the sine and cosine transforms of

the impulse decay response

$$N_\omega = \frac{\int_0^\infty F(t) \sin \omega t \cdot dt}{\int_0^\infty F(t) \cdot dt} \quad (4a)$$

$$D_\omega = \frac{\int_0^\infty F(t) \cos \omega t \cdot dt}{\int_0^\infty F(t) \cdot dt} \quad (4b)$$

Finally, the experimentally determined Θ_ω and M_ω data are related to apparent phase and modulation lifetimes by

$$\tau_{p,\omega} = \theta_\omega / 2\pi\omega \quad (5)$$

and

$$\tau_{M,\omega} = (1/M_\omega^2 - 1)^{1/2} / \omega \quad (6)$$

We have fitted Eqs. (2)–(6) to the observed intensity, phase, and modulation data by numerically integrating (over 10-ps intervals from 0 to 20 ns) Eqs. (2), (4a), and (4b) for values of the two fitting parameters, τ_o and D . We have fixed R_o to be 5.5 Å, which is the value determined in the work by Lakowicz *et al.* [10] and which is approximately the sum of the molecular radii of NATA and O₂. Since the values of R_o and D are highly correlated, we decided to fix R_o rather than have it as a fitting parameter. A program was written in Turbo BASIC, using the nonlinear least-squares algorithm of Bevington [14], to perform the simultaneous fit of intensity and phase data (and modulation data, in some cases) versus [O₂]. The raw phase lifetime, $\tau_{p,\omega}$, and modulation lifetime, $\tau_{M,\omega}$, data are quantities that are easily measured at a single frequency, ω , along with the relative steady-state intensity, F , for the same sample. Standard deviations of 1%, 0.5%, and 0.005 were used for the observed intensity, phase angle, and modulation values, respectively.

RESULTS

In Fig. 1A are shown Stern–Volmer plots for the O₂ quenching of the fluorescence intensity and phase lifetime (at 50 MHz) of NATA in water at 25°C. The Stern–Volmer plots are essentially linear, and the lifetime plot has a slightly lower slope than does the intensity plot (i.e., a very small degree of apparent “static” quenching). The intensity and phase lifetime data sets were simultaneously fitted with the Smoluchowski transient model of Eqs. (2)–(6) by a numerical integration and nonlinear least-squares procedure. With a fixed value of $R_o = 5.5$ Å, we obtained the fit shown with a D value of 2.03×10^{-5} cm²/s. Note that the model pre-

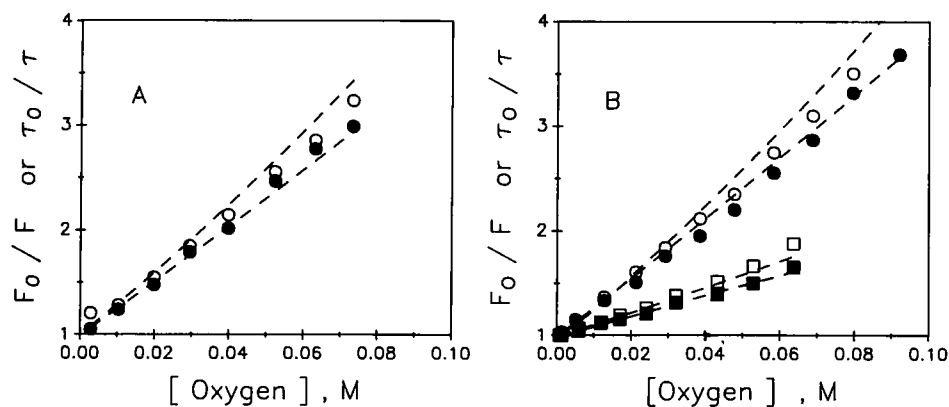


Fig. 1. (A) Intensity (○) and phase lifetime (●) Stern-Volmer plots for the O₂ quenching of NATA in water at 25°C. Lifetime data are phase lifetimes obtained at a modulation frequency of 50 MHz. The dashed lines are a simultaneous fit of Eqs. (2)–(6) to both data sets with R_0 fixed at 5.5 Å, $\tau_0 = 2.75$ ns, and $D = 2.03 \times 10^{-5}$ cm²/s. (B) Intensity (open symbols) and phase lifetime (filled symbols) Stern-Volmer plots for the O₂ quenching of NATA in water (○, ●) at 15°C and in 45% glycerol-water (□, ■) at 15°C. The dashed lines are fits of Eqs. (2)–(6) with $R_0 = 5.5$ Å and with τ_0 and D values given in Table I. A preliminary report of the data in this figure has been published in Ref. 7.

dicts a spread in the intensity and lifetime curves (which would usually be called “static” quenching) and that the data are consistent with this model, although they show less of a spread than the theoretical curves. To test the model we also studied the O₂ quenching of NATA fluorescence at 15°C and at 15°C in a 45% glycerol–water solution. As shown in Fig. 1B, the raw intensity and lifetime data show a certain degree of apparent “static” quenching. The simultaneous fits of intensity and phase lifetime data with Eqs. (2)–(6) adequately describe both types of data. The recovered D values (see Table I) shows the expected decrease as the temperature is increased and as the viscosity is increased. The value of $D = 2.03 \times 10^{-5}$ cm²/s for quenching at 25°C can be compared with literature values for diffusion coefficients. The D for O₂ in aqueous solution at 25°C has been determined by various workers to be between 2.0 and 2.5×10^{-5} cm²/s [18]. Assuming a value of 0.5 – 0.7×10^{-5} cm²/s for NATA (estimated from a D values for a similar-size molecule, *p*-aminobenzoic acid [19]), we arrive at an expected D of 2.7 – 3.2×10^{-5} cm²/s, which compares well with our fitted value of 2.03×10^{-5} cm²/s.

Figure 2 shows similar O₂ quenching data for several single tryptophan-containing proteins. These proteins include ribonuclease T₁, apoazurin, and asparaginase, which contain internal tryptophan residues, and nuclease, for which the tryptophan residue is partially exposed. In each case, the deviation between the intensity and the phase lifetime (at 50 MHz) is significant, which can be described as indicating apparent static quenching. We have also studied the O₂ quenching of monellin and

adrenocorticotropin, which contain partially and fully exposed single tryptophan residues, respectively. For the latter proteins, the deviation between the intensity and the lifetime plots is smaller than in the above-mentioned proteins.

Analysis by the Smoluchowski transient model yields the fits shown in Fig. 2 with the values of the quencher diffusion coefficient listed in Table I. Table I also lists the values of D obtained by Lakowicz *et al.* [10] by analysis of multifrequency phase/modulation lifetime data to the Smoluchowski model and to the radiation boundary model. We note that our fits of Eqs. (2)–(6) assume that the fluorescence decay of the protein, in the absence of quencher, can be adequately described as a single-exponential decay time, τ_0 . For many proteins this will be a crude approximation, but multifrequency phase and modulation data would be needed to extend the analysis to a biexponential description of the decay in the absence of quencher. The strategy in this work has been to make measurements at a single modulation frequency to enable lifetime and intensity measurements to be made rapidly.

The values of D in Table 1 are also converted to quenching rate constant values, k_q , by calculations of the time-independent part of Eq. (1), i.e., $k_q = 4\pi R_0 D N^*$. These k_q values are listed in Table II and range from 0.6×10^9 M⁻¹ s⁻¹ for the tryptophan in apoazurin to 7×10^9 M⁻¹ s⁻¹ for the solvent exposed tryptophan in adrenocorticotropin.⁶ For O₂ quenching of NATA at 25°C the k_q calculated from the fitted D is equal to 8.4×10^9 M⁻¹ s⁻¹. From a traditional analysis of the slope of the Stern–Volmer plot in Fig. 1A, we obtain an apparent k_q

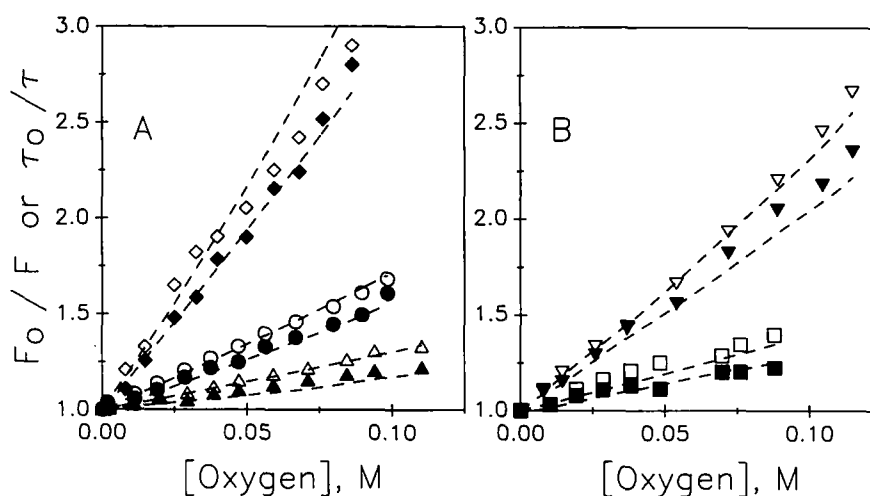


Fig. 2. (A) Intensity (open symbols) and phase lifetime (filled symbols) Stern-Volmer plots for the O_2 quenching of ribonuclease T_1 (\circ , \bullet), asparaginase (Δ , \blacktriangle), and adrenocorticotropin (\diamond , \blacklozenge). (B) Intensity (open symbols) and phase lifetime (filled symbols) Stern-Volmer plots for the O_2 quenching of apozurin (\square , \blacksquare) and nuclease (∇ , \blacktriangledown). Temperature, 20°C ; buffer conditions given in Table I. The dashed lines are simultaneous fits of both intensity and phase data sets with Eqs. (2)–(6) as described in the text. The fitting parameters are given in Table I.

Table II. Oxygen Quenching Rate Constants for Single Tryptophan-Containing Proteins^a

Protein	k_q^o ($\times 10^{-9} M^{-1} s^{-1}$)	Emission λ_{\max} (nm)
Apozurin	0.59	308
Asparaginase	0.66	319
Ribonuclease T_1	1.40	322
Parvalbumin	1.60	316
Nuclease A	1.90	334
fd phage	2.0	328
Monellin	4.2	342
Myelin basic protein	5.9 ^b	340
Gonadotropin	5.6 ^b	340
Melitin		
Tetramer	8.2 ^b	334
Monomer	11.0 ^b	346
Glucagon	8.8 ^b	352
Adrenocorticotropin	7.2	352
NATA	8.4	350

^aValue of k_q calculated from the fitted D values in Table I and Eq. (1) (neglecting the \sqrt{t} term).

^bValues of k_q are taken from Ref. 5. These k_q values were determined from slopes of Stern-Volmer plots for steady-state intensity data. Since such plots will contain an apparent "static" component from the transient term in Eq. (1), k_q from such Stern-Volmer plots will be overestimates.

of 10.0×10^9 and $10.9 \times 10^9 M^{-1} s^{-1}$ from the lifetime and intensity data, respectively. Thus the values of k_q determined from the fits of Eqs. (2)–(6) are slightly lower,

due to the fact that they do not include a contribution from the transient term of the Smolulchowski equation.

DISCUSSION

By slowly bubbling O_2 gas through an aqueous solution in a standard cuvette, we have been able to reduce significantly the equilibration time for O_2 quenching experiments. We are able to collect lifetime quenching data, at about 10 separate O_2 concentrations, in less than 2 h. The stability of the Pockels cell light modulator enables us to measure simply reference phase angles and modulation ratios before and after the measurement of the sample. (On occasion, we have also used the Rayleigh scattered light of the sample as a reference.) Our arrangement also enables a much smaller solution to be used.

For a series of proteins possessing a single tryptophan residue, we find the oxygen k_q to range from 0.6 to $7 \times 10^9 M^{-1} s^{-1}$. The lower end of this range is smaller than the lowest values of k_q previously reported for other proteins. The magnitude of k_q for O_2 quenching does appear to correlate with the solvent exposure of the trp residue in proteins. To illustrate this point, we show in Fig. 3 the correlation between k_q^o and the emission λ_{\max} for the protein and the correlation between the k_q^o for O_2 quenching and the k_q^A for acrylamide quenching

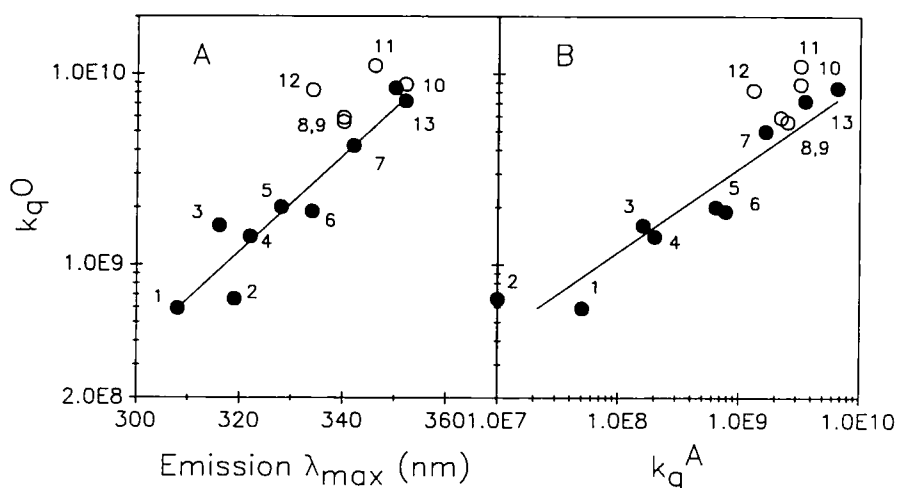


Fig. 3. (A) Comparison of the oxygen quenching k_q^O with the emission λ_{max} for a series of single trp proteins. Filled symbols are from this study and are for an analysis via the Smoluchowski transient model. Open symbols are from previous work in which the k_q^O were determined from slopes of steady-state Stern-Volmer plots. The solid line is drawn through data from this study and has a correlation coefficient of 0.947. (B) Comparison of the oxygen quenching k_q^O and the acrylamide quenching k_q^A for a series of single trp proteins. The proteins are indicated as follows: 1, apoazurin; 2, asparaginase; 3, parvalbumin; 4, RNase T₁; 5, fd phage; 6, nuclease A; 7, monellin; 8, myelin basic protein; 9, gonadotropin; 10, glucagon; 11, melittin monomer; 12, melittin tetramer; and 13, adrenocorticotropin. The k_q^O and k_q^A not reported here are taken from Refs. 5, 11, and 15-17. The solid line is drawn through data from this study and has a correlation coefficient of 0.948.

of the same proteins [11].⁷ The latter quencher is more selective than is the smaller molecular oxygen quencher. The ability of O₂ to diffuse through protein matrices is thus a little more limited than has been previously believed.

The values of k_q for O₂ quenching of fluorescence can be compared to related values for the rate constant for O₂ quenching of the triplet state of tryptophan residues in proteins. From comparison with the latter values reported by Calhoun *et al.* [20] and Ghiron *et al.* [21], the ratio of triplet and singlet oxygen quenching rate constants (k_q^T/k_q^S) is between 0.1 and 0.3; for model indole compounds in nonviscous solutions, the corresponding ratio of triplet-to-singlet O₂ quenching rate constants is 0.4 to 0.7 [21]. This difference in efficiency of triplet and singlet quenching rate constants can be attributed to the spin-statistical factor; Kearns and Stone [22] have argued that this factor can range from 1/9 to 1.0.

⁷ In Fig. 3 and Table II we have included values of k_q^O determined previously by Lakowicz *et al.* [5] using steady-state Stern-Volmer plots. Such analyses yield apparent k_q^O values that are larger than the values we calculate from $k_q^O = 4 \cdot \pi R_0^2 D N'$, since the former k_q^O values include the "static" component, whereas the values calculated from the D (obtained by fits of the transient model) represent only the dynamic quenching component described by the time-independent portion of Eq. (1).

Apparent "static" quenching by O₂ is observed. The ratio of static to dynamic components is as high as 30-80%. This could be interpreted in terms of the weak partitioning of O₂ into the matrix of these proteins. Alternatively, the apparent static quenching can be caused by the transient term of the Smoluchowski equation for the diffusional process. We introduce here a procedure of simultaneously fitting fluorescence intensity and lifetime data to the Smoluchowski model for quenching. We are able to describe the data adequately with reasonable O₂ diffusion coefficients and interaction radius. Thus we find the latter explanation to be more fundamental and we do not believe that it is necessary to propose the sequestering of O₂ molecules into the protein (other than those molecules that enter and exit by diffusion) to describe the total quenching data.

The transient model that we have used is the Smoluchowski \sqrt{t} model. Lakowicz and co-workers have argued that a slightly more complicated model, known as the radiation boundary condition model, must be used to fit intensity decay data adequately for some quenching reactions [9,10]. Very recently, Lakowicz and co-workers have also demonstrated that fits of time-resolved fluorescence quenching data [e.g., for the CBr₄ quenching of *p*-bis[2-(5-phenyloxazolyl)]benzene and the acrylamide quenching of NATA in viscous solutions] are improved by including a distance dependence to the transient

quenching model [23,24]. The latter studies have generally involved isotropic solutions. With proteins having internal trp residues, the diffusional process of quencher toward a trp residue is intrinsically anisotropic. There will be different diffusional barriers for the approach of quencher from different directions, i.e., some diffusional paths will be easier than others. In recognition of this structural anisotropy around a trp residue, and in recognition that the diffusion process may in some cases be better modeled as a two-step process (diffusion through the low solvent to the edge of the protein and then diffusion through the protein matrix [7]), we have opted to fit the data only in terms of the simplest Smoluchowski transient model. As Figs. 1 and 2 show, this transient model describes the general features of the intensity and lifetime Stern-Volmer plots and enables determination of the quencher diffusion coefficient, D , without the need to invoke an additional "static" quenching component.

ACKNOWLEDGMENTS

We express appreciation to Dr. David Jameson, University of Hawaii, for loaning us his oxygen pressure bomb. We also thank Dr. Frederick Walz, Jr., Kent State University, Dr. R. Webster, Duke University, and Dr. R. O. Fox, Yale University, for providing us with protein samples. This research was supported by NSF Grant DMB 91-06377 to M.R.E.

REFERENCES

1. J. R. Lakowicz, and G. Weber (1973) *Biochemistry* **12**, 4171-4178.
2. E. Gratton, D. M. Jameson, G. Weber, and B. Alpert (1984) *Biophys. J.* **45**, 789-794.
3. D. M. Jameson, E. Gratton, G. Weber, and B. Alpert (1984) *Biophys. J.* **45**, 795-803.
4. D. B. Calhoun, J. M. Vanderkooi, G. V. Woodrow III, and S. W. Englander (1984) *Biochemistry* **22**, 1526-1532.
5. J. R. Lakowicz, B. P. Maliwal, H. Cherek, and A. Balter (1983) *Biochemistry* **22**, 1741-1752.
6. M. R. Eftink, and K. Hagaman (1985) *Biophys. Chem.* **22**, 173-180.
7. M. R. Eftink (1990) *Proc. SPIE* **1204**, 406-414.
8. M. R. Eftink, and C. A. Ghiron (1989) *Photochem. Photobiol.* **50**, 425-428.
9. J. R. Lakowicz, M. L. Johnson, I. Gryczynski, N. Joshi, and G. Laczo (1987) *J. Phys. Chem.* **91**, 3277-3285.
10. J. R. Lakowicz, N. B. Joshi, M. L. Johnson, H. Szmecinski, and I. Gryczynski (1987) *J. Biol. Chem.* **262**, 10907-10910.
11. M. R. Eftink (1991) in J. R. Lakowicz (Ed.), *Topics in Fluorescence Spectroscopy, Vol. 2. Theory, Principles and Applications*, Plenum Press, New York, pp. 53-126.
12. J. A. Blaszkak, D. R. McMillin, A. T. Thornton, and D. L. Tennant (1983) *J. Biol. Chem.* **258**, 9886-9892.
13. J. R. Lakowicz, and G. Weber (1973) *Biochemistry* **12**, 4161-4170.
14. P. R. Bevington (1969) *Data Reduction and Error Analysis for Physical Sciences*, McGraw-Hill, New York, Chap. 11.
15. J. R. Lakowicz, B. Maliwal, H. Cherek, and A. Balter (1983) *Biochemistry* **22**, 1741-1752.
16. M. R. Eftink, and C. A. Ghiron (1984) *Biochemistry* **23**, 3891-3899.
17. M. R. Eftink (1983) *Biophys. J.* **43**, 323-334.
18. D. M. Himmelblau (1964) *Chem. Rev.* **64**, 527-550.
19. *CRC Handbook of Chemistry and Physics*, 51st ed. (1970) CRC, Boca Raton, FL, p. F-47.
20. D. B. Calhoun, S. W. Englander, W. W. Wright, and J. M. Vanderkooi (1988) *Biochemistry* **27**, 8466-8474.
21. C. A. Ghiron, M. Basin, and R. Santus (1988) *Biochim. Biophys. Acta* **957**, 207-216.
22. D. R. Kearns, and A. J. Stone (1971) *J. Chem. Phys.* **55**, 3383-3389.
23. J. R. Lakowicz, J. Kusba, H. Szmecinski, M. L. Johnson, and I. Gryczynski (1993) *Chem. Phys. Lett.* **206**, 455-463.
24. J. R. Lakowicz, B. Zelent, I. Gryczynski, J. Kusba, and M. L. Johnson (1994) *SPIE Symp. Proc.* **2137** (in press).